Performance of Ultra Wideband SSMA Using Time-Hopping and M-ary PPM

Fernando Ramírez-Mireles, member, IEEE

Abstract— **Wireless spread spectrum multiple-access (SSMA) using time hopping and block waveform encoded (M-ary) pulse position modulated (PPM) signals is analyzed. For different M-ary PPM signal designs the multiple-access performance in free-space propagation conditions is analyzed in terms of the number of users supported by the system for a given bit error rate, signal to noise ratio, bit transmission rate and number of signals in the M-ary set. Processing gain and number of simultaneous users are described in terms of system parameters. Tradeoffs between performance and receiver complexity are discussed. Upper bounds on both the maximum number of users and the total combined bit transmission rate are investigated. This analysis is applied to ultra-wideband impulse radio modulation. In this modulation, the communications waveforms are practically realized using subnanosecond impulse technology. A numerical example is given that shows that impulse radio modulation is theoretically able to provide multiple-access communications with a combined transmission capacity of hundreds of Megabits per second at bit error rates in the range 10^{-4} to 10^{-7} using receivers of moderate complexity.**

Keywords— **Ultra-wideband impulse radio modulation, spread spectrum multiple-access, time hopping, pulse position modulation.**

I. Introduction

SPREAD spectrum multiple-access (MA) communications using time hopping (TH) and binary PPM was recently proposed in [1] [2]. The proposed scheme is a baseband modulation where the signals consist of trains of time-shifted pulses. Data is transmitted using binary PPM at a rate of many pulses per symbol, and MA capability is achieved using spread spectrum TH[1].

When these TH PPM signals are practically realized using subnanosecond impulse signal technology, this ultra-wideband SSMA technique is known in the literature as impulse radio modulation. In this case, the range of frequencies occupied by the TH PPM signals goes from a few hundreds of Kilohertz up to a few Gigahertz. The ultra-wideband nature of this modulation can potentially facilitate the construction of relatively simple, low-cost, low-power transceivers that can be used for license-free, short range, high speed MA communications over indoor and other dense-multipath wireless channels [1] [2] [5] [6] [7]. Although there are spectrum compatibility issues related with the coexistence between this ultra-wideband modulation and the numerous narrowband waveforms within that bandwidth, the technical feasibility of impulse radio modulation has already been demonstrated [1] [5].

The work in [2] studied MA performance assuming free space propagation conditions and additive white Gaussian noise (AWGN). The analysis assumed that binary PPM signals based on binary time-shift-keyed pulses are coherently detected using a single-channel correlation receiver. The analysis in [2] is quite similar to the analysis for code division multiple-access made in [8] and is based on the fact that both designs use single-channel correlation receivers for coherent detection of the bit waveform.

This paper extends the results in [2] to investigate the use of M-ary PPM signals to improve the MA performance for a given number of users and data transmission rate, or to increase the number of users supported by the system for a given MA performance and data transmission rate [9]. This results can also be applied to increase the data transmission rate supported by the system without degrading the MA performance for a given number of users [10]. The results that follows, as well as the results in [2], are valid for a fairly general class of TH PPM system, not necessarily of ultra-wideband nature.

II. Channel, signals and multiple-access interference models

A. The basic pulse

The signal $w(t)$ is the basic pulse used to convey information. It has duration T_w, two-sided 3 dB bandwidth W, energy $E_w = \int_{-\infty}^{\infty}[w(\xi)]^2 d\xi$, and normalized signal correlation function

$$\gamma_w(\tau) \triangleq \frac{1}{E_w}\int_{-\infty}^{\infty} w(t)w(t-\tau)dt > -1$$

for all τ. The minimum value of $\gamma_w(\tau)$ is denoted $\gamma_{\min}$, and $\tau_{\min}$ denotes the smallest value of τ in $(0, T_w]$ such that $\gamma_{\min} = \gamma_w(\tau_{\min})$.

B. Channel

The channel model used in this MA performance analysis has free-space propagation conditions. The effect of the antenna system in the UWB transmitted pulse is modeled as a differentiation operation. The transmitted pulse is $w_{\text{TX}}(t) \triangleq \int_{-\infty}^{t} w(\xi)d\xi$ and the received pulse is $Aw(t-\tau) + n(t)$. The constants A and τ represent the attenuation and propagation delay, respectively, that the

This research was done at the Communication Sciences Institute, University of Southern California, and was supported in part by the Joint Services Electronics Program under contract F49620-94-0022.

Dr. Ramírez's is now with Aware Inc., Strategic Technologies Group, Lafayette, CA. His E-mail is ramirezm@ieee.org

[1]Spread spectrum using PPM has been analyzed previously [3] [4]. One novel aspect of [1] [2] is the combination of TH with PPM.

signal experiences over the link path between the transmitter and receiver. The noise $n(t)$ is AWGN with two-sided power density $N_o/2$.

C. TH PPM signals

The TH PPM signal conveying information exclusively in the time shifts is

$$x^{(\nu)}(t) = \sum_{k=0}^{\infty} w(t - kT_f - c_k^{(\nu)} T_c - \delta^k_{d^{(\nu)}_{\lfloor k/N_s \rfloor}}). \qquad (1)$$

The superscript (ν), $1 \le \nu \le N_u$, indicates user-dependent quantities, where N_u is the number of simultaneous active users. The index k is the number of time hops that the signal $x^{(\nu)}(t)$ has experienced, and also the number of pulses that has been transmitted. The T_f is the frame (pulse repetition) time and equals the average time between pulse transmissions. The notation $\lfloor q \rfloor$ denotes the integer part of q.

The $\{c_k^{(\nu)}\}$ is the pseudo-random time-hopping sequence assigned to user ν. It is periodic with period N_p (i.e., $c^{(\nu)}_{k+lN_p} = c_k^{(\nu)}$, for all k, l integers) and each sequence element is an integer in the range $0 \le c_k^{(\nu)} \le N_h$. For a given time shift parameter T_c, the time hopping code provides an additional time shift to the pulse in every frame, each time shift being a discrete time value $c_k^{(\nu)} T_c$, with $0 \le c_k^{(\nu)} T_c < N_h T_c$.

The time shift corresponding to the data modulation is $\delta^k_{d^{(\nu)}_{\lfloor k/N_s \rfloor}} \in \{\tau_1 = 0 < \tau_2 < \ldots < \tau_\eta\}$, with $\eta \ge 2$ an integer. The data sequence $\{d_m^{(\nu)}\}$ of user ν is an M-ary symbol stream, $1 \le d_m^{(\nu)} \le M$, that conveys information in some form. The system under study uses fast time hopping, which means that there are $N_s > 1$ pulses transmitted per symbol. The data symbol changes only every N_s hops. Assuming that a new data symbol begins with pulse index $k = 0$, the data symbol index is $\lfloor k/N_s \rfloor$.

In general, M, η and N_s are system design parameters. The specific values of these parameters depends on performance requirements and implementation considerations, among other criteria. The relation between them depends also on the particular signal design under consideration.

To avoid overlapping of pulses belonging to different frames, we assume that $N_h T_c + \tau_\eta + T_w < T_f$. In practical realizations of impulse radio modulation, the pulse duration satisfies $T_w << T_f$, the maximum time shift value satisfies $\tau_\eta < T_f/2$ and N_s is usually in the order of hundreds. The values of N_h and T_c are discussed in section II-E.

If we define

$$H_m^{(\nu)}(t) \triangleq \sum_{k=mN_s}^{(m+1)N_s - 1} T_c \, c_k^{(\nu)} p(t - kT_f), \qquad (2)$$

$$p(t) = \begin{cases} 1, & \text{if } 0 \le t \le T_f \\ 0, & \text{otherwise} \end{cases},$$

and

$$S_i(t) \triangleq \sum_{k=0}^{N_s - 1} w(t - kT_f - \delta_i^k) \qquad (3)$$

for $i = 1, 2, \ldots, M$, then (1) can be rewritten

$$\begin{aligned} x^{(\nu)}(t) &= \sum_{m=0}^{\infty} S_{d_m^{(\nu)}}(t - mN_s T_f - H_m^{(\nu)}(t)) \\ &\triangleq \sum_{m=0}^{\infty} X^{(\nu)}_{m, d_m^{(\nu)}}(t), \end{aligned}$$

where m indexes the transmitted symbols. Hence, the user's information signal $x^{(\nu)}(t)$ is composed of a sequence of communications waveforms $X^{(\nu)}_{m, d_m^{(\nu)}}(t)$, $m = 0, 1, 2, \ldots$, where each $X^{(\nu)}_{m, d_m^{(\nu)}}(t)$ is a fast-hopped version of one of the M possible PPM symbol waveforms $S_i(t)$ in (3).[2] A single symbol waveform has duration $T_s \triangleq N_s T_f$. For a fixed T_f, the M-ary symbol rate $R_s = T_s^{-1}$ determines the number N_s of pulses that are modulated by a given symbol. Note that when the hopping function $H_m^{(\nu)}(t)$ in (2) is known (i.e., the receiver is synchronized), the signals $\{S_i(t)\}$ and $\{X^{(\nu)}_{m,i}(t)\}$ both have the same correlation properties, i.e.,

$$\begin{aligned} R_{ij} &\triangleq \int_{-\infty}^{\infty} X^{(\nu)}_{m,i}(\xi)\, X^{(\nu)}_{m,j}(\xi)\, d\xi \\ &= \int_{-\infty}^{\infty} S_i(\xi)\, S_j(\xi)\, d\xi \\ &= E_w \sum_{k=0}^{N_s - 1} \gamma_w(\delta_i^k - \delta_j^k), \end{aligned}$$

since the pulses are non overlapping. The energy in the i^{th} signal $X^{(\nu)}_{m,i}(t)$ is $E_S = R_{ii} = N_s E_w$, and the normalized correlation value is

$$\alpha_{ij} \triangleq \frac{R_{ij}}{E_S} = \frac{1}{N_s} \sum_{k=0}^{N_s - 1} \gamma_w(\delta_i^k - \delta_j^k) \ge \gamma_{\min}.$$

D. M-ary PPM signal sets

The PPM signal $S_i(t)$ in (3) represents the i^{th} signal in an ensemble of M information signals, each signal completely identified by the pulse shape $w(t)$ and the sequence of time shifts $\{\delta_i^k\}$, $k = 0, 1, 2, \ldots, N_s - 1$. In this paper we will focus in M-ary PPM sets with the greatest practical interest, namely orthogonal (OR), equally correlated (EC) and N-orthogonal (NO) signal sets[3].

In general, the proposed signal designs have the virtue that the structure of the M-ary autocorrelation matrix is preserved for different $w(t)$. This is important because $w(t)$ is, in general, a non standard pulse, and these signal design

[2]The signal $S_i(t)$ is the received signal corresponding to the transmitted signal $\int_{-\infty}^{t} S_i(\xi) d\xi = \sum_{k=0}^{N_s - 1} w_{\text{TX}}(t - kT_f - \delta_i^k)$.

[3]For the N-orthogonal signal designs a value of $N = 2$ was used. For other values of N (the number of signals in each orthogonal dimension) see [10].

Type of signal	Time shift pattern $\{\delta_i^k\}$ $i = 1, 2, \ldots, M$ $k = 0, 1, \ldots, N_s - 1$	normalized correlation coefficient
OR	$\delta_i^k = [(k+i-1) \bmod M] T_{\rm OR}$ $T_{\rm OR} = 2T_w$	$\alpha_{ij}^{(\rm OR)} = \begin{cases} 1, & i = j \\ 0, & i \neq j \end{cases}$
EC	$\delta_i^k = a_i^k \tau_2$ $\tau_2 \in (0, T_w]$ $a_i^k \in \{0, 1\}$	$\alpha_{ij}^{(\rm EC)} = \begin{cases} 1, & i = j \\ \lambda, & i \neq j \end{cases}$ $\lvert\lambda\rvert < 1$
NO1	$\delta_i^k = \tau_1 + \left[(k + 2\tilde{I}) \bmod L\right] T_{\rm NO1}$ $L \triangleq \lfloor \frac{M}{2} \rfloor$ $I = i - \lfloor \frac{i-1}{2} \rfloor 2$ $\tilde{I} \triangleq \lfloor \frac{i-1}{2} \rfloor$ $T_{\rm NO1} \triangleq \tau_2 + T_{\rm OR}$ $0 = \tau_1 < \tau_2 < T_w$	$\alpha_{ij}^{(\rm NO1)} = \begin{cases} 1, & i = j \\ 0, & \lfloor \frac{i-1}{2} \rfloor \neq \lfloor \frac{j-1}{2} \rfloor \\ \beta_{ij}, & \lfloor \frac{i-1}{2} \rfloor = \lfloor \frac{j-1}{2} \rfloor \end{cases}$ $\beta_{ij} = \gamma_w(\tau_J - \tau_I)$ $J = j - \lfloor \frac{j-1}{2} \rfloor 2$
NO2	$\delta_i^k = a_i^k \tau_2 + \left[(k + 2\tilde{I}) \bmod L\right] T_{\rm NO2}$ $T_{\rm NO2} \triangleq \tau_2 + T_{\rm OR}$ $0 = \tau_1 < \tau_2 < T_w$	$\alpha_{ij}^{(\rm NO2)} = \begin{cases} 1, & i = j \\ 0, & \lfloor \frac{i-1}{2} \rfloor \neq \lfloor \frac{j-1}{2} \rfloor \\ \lambda, & \lfloor \frac{i-1}{2} \rfloor = \lfloor \frac{j-1}{2} \rfloor \end{cases}$

TABLE I

TIME SHIFT PATTERNS AND NORMALIZED CORRELATION VALUES OF THE M-ARY PPM SIGNALS UNDER STUDY. ORTHOGONAL (OR), EQUALLY CORRELATED (EC), N-ORTHOGONAL DESIGN 1 (NO1) AND N-ORTHOGONAL DESIGN 2 (NO2).

reduce the dependence of the MA performance on the shape of $w(t)$. The time shift patterns defining each M-ary PPM signal set and their respective correlation properties are studied in detail in [10] and summarized in table I. In the EC case the a_i^k is a $0, 1$ pattern representing the $i^{\rm th}$ cyclic shift, $i = 1, 2, \ldots, M$, of an m-sequence [13] of length $N_s = 2^m - 1$, $m \geq 1$, and $N_s \geq M$.

As pointed out by one of the reviewers, PPM has been widely used in optical communications. Hence, previous results in PPM signal design such as [11] [12] could also been considered for the M-ary signal sets. One notorious difference with previous results is that in [11] [12] the values of δ_j^k, are constrained to be an integer multiple of T_w, where as in the present work δ_j^k can actually be less that T_w to take advantage of the negative correlation properties of $w(t)$.

E. Multiple-access interference model

In this analysis, performance computation is based on signal-to-noise ratios (SNR) averaged over the TH sequence variables and propagation delay variables. It is a formidable task to develop exact generalized results that are meaningful for the MA performance. In order to facilitate the analytical treatment, the following assumptions were made:

(a) The signals $x^{(\nu)}(t - \tau^{(\nu)})$, for $\nu = 1, 2, \ldots, N_u$, and the noise $n(t)$ are all assumed to be independently generated.

(b) To estimate performance without choosing a specific TH sequence family, we use purely random TH sequences, i.e., the elements $\{c_k^{(\nu)}\}$, for $\nu = 1, 2, 3, \ldots, N_u$, and for all k, are independent, identically distributed (i.i.d.) random variables, with each $c_k^{(\nu)}$ uniformly distributed on the interval $[0, N_h]$. The results of the analysis are independent of the specific value of $N_h T_c$, as long as the condition (f) is valid. To insure that no hopping code random variable $c_k^{(\nu)}$ occur more than once in a symbol time, we assume that $N_s \leq N_p$. For many hops to occur in a symbol time, we further assume that $N_s >> 1$.

(c) Asynchronous radio transmission dictates that the time delays $\tau^{(\nu)}$, $\nu = 2, 3, \ldots, N_u$, are i.i.d random variables. The magnitude of $\tau^{(\nu)}$ spans many frames T_f, hence we can write $\tau^{(\nu)} = \Phi T_f + \phi$. Hence Φ is the value of $\tau^{(\nu)}$ rounded to the nearest frame time, and $T_f/2 \leq \phi < T_f/2$ is the error in this rounding process. Since ϕ is a round-off error of a large

random variable, it is reasonable to assume that ϕ is uniformly distributed over it's range. A model for Φ won't be needed because the final calculations are independent of it, as long as the condition (f) is valid. We also assume that the transmission time differences $\tau^{(\nu)} - \tau^{(1)}$, $\nu = 2, 3, \ldots, N_u$, are i.i.d. random variables, with $\tau^{(\nu)} - \tau^{(1)} \bmod T_f$ being uniformly distributed on $[0, T_f)$.

(d) Since the received signal $w(t)$ is modeled as the derivative of the transmitted signal $w_{\rm TX}(t)$, we assume that the pulse $w(t)$ satisfies the relation $\int_{-\infty}^{\infty} w(\xi)\, d\xi = 0$.

(e) In this analysis we assume that τ_η is smaller than both the range of the time uncertainty parameter ϕ and the time hopping window width $N_h T_c$. We further assume that data modulation in the signals of the other $N_u - 1$ users has no significant effect on the calculation of multiple-access interference statistics for user one (the desired user). Hence, $\delta^k_{d_m^{(\nu)}} = 0$ for $\nu = 2, 3, \ldots, N_u$, and all k and m.

(f) To further simplify the analysis we assume that the time interval over which the pulse $w(t)$ can be time hopped is less than a half a frame time, so that $N_h T_c < (T_f/2) - \epsilon$, where $\epsilon \triangleq 2(T_w + \tau_\eta)$ is two times the duration of $w(t) - w(t - \tau_\eta)$.

III. Receiver signal processing

When N_u links are active in this MA system, the received signal $r(t)$ can be modeled as

$$r(t) = \sum_{\nu=1}^{N_u} A^{(\nu)} x^{(\nu)}(t - \tau^{(\nu)}) + n(t), \tag{4}$$

where $A^{(\nu)}$ is the attenuation of user ν's signal over the channel, $\tau^{(\nu)}$ represents time asynchronisms between the clocks of the transmitter of user ν and the receiver, and the signal $n(t)$ represents non MA interference modeled as AWGN.

Let's assume that the receiver wants to demodulate the signal of user $\nu = 1$ corresponding to the $m^{\rm th}$ data symbol $d_m^{(1)}$, where $d_m^{(1)}$ is one of M equally-likely symbols. The received signal $r(t)$ in (4) can be viewed as

$$r(t) \;=\; A^{(1)} X^{(1)}_{m, d_m^{(1)}}(t - \tau^{(1)}) + n_{\rm TOT}(t),\; t \in \mathcal{T}_m, \tag{5}$$

where

$$\mathcal{T}_m \triangleq [m N_s T_f + \tau^{(1)}, (m+1) N_s T_f + \tau^{(1)}),$$

and

$$n_{\rm TOT}(t) \triangleq \sum_{\nu=2}^{N_u} A^{(\nu)} x^{(\nu)}(t - \tau^{(\nu)}) + n(t).$$

When the receiver is perfectly synchronized to the first user signal, i.e., having learned the value of $\tau^{(1)}$ (or at least $\tau^{(1)} \bmod N_p T_f$), the receiver is able to determine the sequence $\{\mathcal{T}_m\}$ of time intervals, with interval $\mathcal{T}_m$ containing the waveform representing data symbol $d_m^{(1)}$. In this case the detection problem becomes the time-shift-coherent detection of M equal-energy, equally-likely signals in the presence of multiple-access interference in addition to AWGN. The corresponding optimal receiver (multi-user detector) is a complicated structure that takes advantage of all of the receiver's knowledge regarding the characteristics of the multiple-access interference [14] [15].

A much simpler receiver to analyze is the the conventional M-ary correlation receiver [16]. The use of this receiver for time-shift-coherent detection of M equal-energy, equally-likely signals in the presence of mean-zero Gaussian interference in addition to AWGN is well justified when $N_u >> 1$ and $N_s >> 1$. In both cases we can use the assumptions made in section II-E to invoke the Central Limit Theorem [17] to conclude that the net effect of the multiple-access interference produced by the undesired users at the output of the desired user's correlation receivers can be modeled as zero-mean Gaussian random variables. Notice that in time hopping, at most a few pulses simultaneously are present in any given time slot, and that we are applying the Gaussian assumption to the decision variables, as opposed to the received waveform

The M-ary correlation receiver consists of M filters matched to the signals $\{X^{(1)}_{m,j}(t - \tau^{(1)})\}$, $j = 1, 2, \ldots, M$, $t \in \mathcal{T}_m$, followed by samplers and a decision circuit that selects the maximum among the decision variables

$$y_j \;=\; \int_{t \in \mathcal{T}_m} r(t)\; X^{(1)}_{m,j}(t - \tau^{(1)})\; dt\;,\; j = 1, 2, \ldots, M.$$

This receiver is illustrated in Fig. 1. As discussed in [10], this receiver can be greatly simplified for different M-ary PPM signal designs. These simplification results are summarized in tables II and III.

The performance of this receiver can be studied using standard communications techniques [16]. The union bound for the symbol error probability (SER) for time-shift-coherent detection of the TH PPM signals is

$$\begin{aligned} {\rm UBP}_e(N_u) \;&\triangleq\; \tfrac{1}{M} \sum_{i=1}^{M} \sum_{\substack{j=1 \\ i \neq j}}^{M} \\ &\qquad Q\left(\sqrt{\log_2(M) \mathbf{SNRb}^{(j,i)}_{\rm out}(N_u)} \right), \end{aligned} \tag{6}$$

where $Q(\cdot)$ is the Gaussian tail integral,

$$\begin{aligned} \mathbf{SNRb}^{(j,i)}_{\rm out}(N_u) \;=\; &\left[\left[\mathbf{SNRb}^{(j,i)}_{\rm out}(1) \right]^{-1} + \right. \\ &\left. \left[\frac{1}{R_b} \frac{\mu(j,i)/T_f}{\sum_{\nu=2}^{N_u} \left(\frac{A^{(\nu)}}{A^{(1)}} \right)^2} \right]^{-1} \right]^{-1}, \end{aligned} \tag{7}$$

$i \neq j$, is the output bit SNR observed in the presence of $N_u - 1$ other users, and

$$\mu(j,i) \;\triangleq\; \frac{\left[\sum_{k=0}^{N_s - 1} m_w(\delta^k_j, \delta^k_j, \delta^k_i) \right]^2}{N_s \sum_{k=0}^{N_s - 1} \sigma^2_w(\delta^k_j, \delta^k_i)} \tag{8}$$

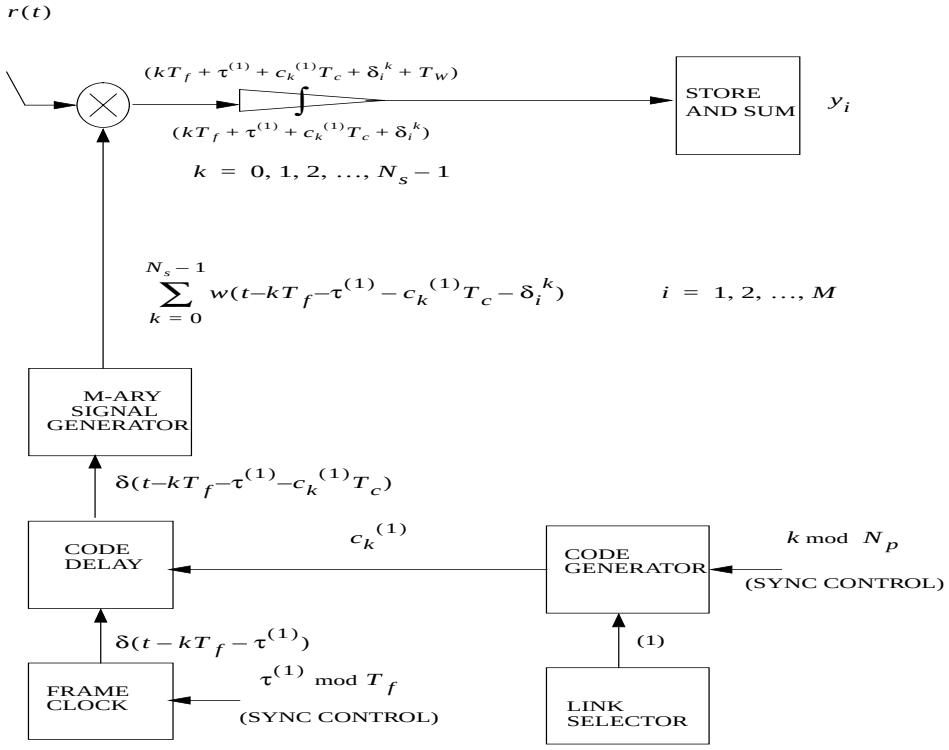

Fig. 1. This diagram shows the M-ary correlation receiver for the TH PPM signals.

is a normalized SNR parameter defined in terms of the pulse shape $w(t)$ and the data modulation time shifts $\{(\delta_j^k, \delta_i^k)\}$, with

$$\sigma_w^2(\theta,\eta) \triangleq T_f^{-1}\int_{-\infty}^{\infty} m_w^2(\varsigma,\theta,\eta)\,d\varsigma, \tag{9}$$

and

$$\begin{aligned} m_w(\varsigma,\theta,\eta) &\triangleq \int_{-\infty}^{\infty} w(\rho-\varsigma)\,[w(\rho-\theta)-w(\rho-\eta)]\,d\rho \\ &= E_w\left[\gamma_w(\varsigma-\theta)-\gamma_w(\varsigma-\eta)\right]. \end{aligned} \tag{10}$$

In (7) we have use the fact that the bit transmission rate $R_b = \log_2(M)/T_s = \log_2(M)/N_sT_f$. Note that $\mathbf{SNRb}_{\text{out}}^{(j,i)}(N_u)$ is smaller than the smallest of $\mathbf{SNRb}_{\text{out}}^{(j,i)}(1)$ and $\frac{1}{R_b}\frac{\mu(j,i)/T_f}{\sum_{\nu=2}^{N_u}\left(\frac{A^{(\nu)}}{A^{(1)}}\right)^2}$. The procedure to calculate (7), (8), (9) and (10) is described in detail in [10].

If only the desired transmitter is active, then

$$\mathbf{SNRb}_{\text{out}}^{(j,i)}(1) = \frac{1}{\log_2(M)}\frac{(A^{(1)})^2E_s[1-\alpha_{ij}]}{N_o} \tag{11}$$

is equivalent to the output bit SNR that one might observe in single-link communications (one user bit SNR).

Given the pulse $w(t)$, the proper signal design depends on the good choice of the data modulation time shifts $\{(\delta_j^k, \delta_i^k)\}$. When $N_u = 1$ or when the AWGN dominates, the values $\{(\delta_j^k, \delta_i^k)\}$ should be chosen to maximize $\mathbf{SNRb}_{\text{out}}^{(j,i)}(1)$ in (11). On the other hand, when MA interference dominates, the $\mu(j,i)$ is the quantity that should be maximized by the proper choice of $\{(\delta_j^k, \delta_i^k)\}$.

IV. MA performance analysis

In this section we elaborate useful relations between bit error rate, signal-to-noise power ratio, number of simultaneous active users, bit transmission rate, and number of signals in the block waveform set.

A. MA BER performance and $\mathbf{SNRb}_{\text{out}}^{(j,i)}(N_u)$

The substitution of the bit SNR $\mathbf{SNRb}_{\text{out}}^{(j,i)}(N_u)$ in (7) into the $\text{UBP}_e(N_u)$ in (6) will provide the desired relation between SER, bit SNR, N_u, R_b and M.

More
insight can be obtained if we rewrite $\mathbf{SNRb}_{\text{out}}^{(j,i)}(N_u)$ in

Type of signal	calculation of decision variables
any	$y_j = \int_0^{N_s T_f} x(t)\, S_j(t)\, dt$ $= \sum_{k=0}^{N_s-1} \int_{kT_f}^{(k+1)T_f} x(t)\, w(t-kT_f-\delta_j^k)\, dt$
OR	$y_j = \sum_{k=0}^{N_s-1} \sum_{q=0}^{M-1} \delta_{q,[(k+j-1) \bmod M]}\, z(k,q)$ $z(k,q) \triangleq \int_{kT_f+qT_{\rm OR}}^{kT_f+(q+1)T_{\rm OR}} x(t)\, w(t-kT_f-qT_{\rm OR})\, dt$
EC	$y_j = \sum_{k=0}^{N_s-1} \sum_{m=1}^{2} \delta_{(m-1),a_j^k}\, z_m(k)$ $z_m(k) \triangleq \int_{kT_f}^{kT_f+T_w+\tau_m} x(t)\, w(t-kT_f-\tau_m)\, dt$ $m = 1,2$
NO1	$y_j = \sum_{k=0}^{N_s-1} \sum_{q=0}^{L-1} \delta_{q,[(k+2\lfloor \frac{j-1}{2} \rfloor) \bmod L]}\, z_J(k,q)$ $z_J(k,q) \triangleq \int_{kT_f+qT_{\rm NO1}}^{kT_f+(q+1)T_{\rm NO1}} x(t)\, w(t-kT_f-\tau_J-qT_{\rm NO1})\, dt$ $J = j-2\lfloor \frac{j-1}{2} \rfloor,\ 1 \le J \le N$
NO2	$y_j = \sum_{k=0}^{N_s-1} \sum_{q=0}^{L-1} \sum_{m=1}^{2} \delta_{(m-1),a_j^k}\, z_m(k,q)$ $z_m(k,q) \triangleq \int_{kT_f+qT_{\rm NO2}}^{kT_f+(q+1)T_{\rm NO2}} x(t)\, w(t-kT_f-\tau_m-qT_{\rm NO2})\, dt$ $m = 1,2$

TABLE II

CALCULATION OF DECISION VARIABLES y_j CAN BE SIMPLIFIED TO GET A RECEIVER OF REDUCED COMPLEXITY. FOR CLARITY WE USE $S_i(t)$ INSTEAD OF $X_{m,i}^{(1)}(t)$. THE $\delta_{q,q'}$ IS THE KRONECKER DELTA.

(7) as

$$\mathbf{SNRb}_{\rm out}^{(j,i)}(N_u) = \frac{(A^{(1)})^2 E_b(1-\alpha_{ji})}{N_o + N_{\rm MA}(j,i)}, \qquad (12)$$

where $E_b \triangleq E_s/\log_2(M)$ is the energy per bit,

$$N_{\rm MA}(j,i) \triangleq \sum_{\nu=2}^{N_u} N_{\rm MA}^{(\nu)}(j,i)$$

is the *equivalent power spectral density level* of the total multiple-access interference, and

$$N_{\rm MA}^{(\nu)}(j,i) \triangleq \frac{(A^{(\nu)})^2\, [E_b(1-\alpha_{ji})]}{G_{ji}} \qquad (13)$$

is the contribution corresponding to the $\nu^{\rm th}$ user, $\nu = 2,3,\ldots,N_u$. The $\mathbf{SNRb}_{\rm out}^{(j,i)}(N_u)$ in (12) clearly indicates that there is an increase in the total effective noise power spectrum density produced by all the other users at the front end of the desired user's receiver. The $N_{\rm MA}^{(\nu)}(j,i)$ in (13) clearly indicates that the level of the MA interference is inversely proportional to the *spreading gain factor*

$$G_{ji} \triangleq (\mu(j,i)/T_f)/R_b. \qquad (14)$$

We can now evaluate $\mathbf{SNRb}_{\rm out}^{(j,i)}(N_u)$ in (12) for the block waveform encoding PPM signal sets considered in section II-D. This requires the calculation of the interference level $N_{MA}^{(\nu)}(j,i)$ in (13) for each signal set. The details of this calculation are given in [10]. Table IV presents the main results.

The SER can be transformed to BER depending on the particular signal design under consideration. Table V shows the union bound on BER, denoted $\rm UBP_b$, for the four PPM signal designs under consideration. These results are based in expression derived in [10].

B. MA degradation factor and N_u.

In order to simplify this analysis, let's assume that the signals are equally correlated. For these signals, the parameters in (7) do not depend on the pair of index (j,i),

Signal set	Maximum number of signals	Dependence of α_{ij} on $\gamma_w(\tau)$	Receiver complexity (correlators)
OR	$\lfloor \frac{T_f}{T_{\rm OR}} \rfloor$	independent of $\gamma_w(\tau)$	1
EC	N_s	depends on $\gamma_{\rm min}$	2
NO1	$2\lfloor \frac{T_f}{T_{\rm NO1}} \rfloor$	depends on $\gamma_w(\tau)$	2
NO2	$N_s \lfloor \frac{T_f}{T_{\rm NO2}} \rfloor$	depends on $\gamma_{\rm min}$	2

TABLE III
RECEIVER COMPLEXITY COMPARISON AMONG SIGNAL SETS

and (7) can be rewritten

$$\mathbf{SNRb}_{\rm out}(N_u) = \frac{\mathbf{SNRb}_{\rm out}(1)}{1+\mathbf{SNRb}_{\rm out}(1)\left[\frac{G}{\sum_{\nu=2}^{N_u}\left(\frac{A^{(\nu)}}{A^{(1)}}\right)^2}\right]^{-1}}, \quad (15)$$

where

$$G = (\mu/T_f)/R_b. \quad (16)$$

Recall that $\mathbf{SNRb}_{\rm out}(1)$ is the bit SNR value when only user one is active, and that $\mathbf{SNRb}_{\rm out}(N_u) < \mathbf{SNRb}_{\rm out}(1)$ is the actual bit SNR when other N_u-1 users are also active in the system. Let's define $\mathbf{SNRb}_{\rm spec}$ to be the specified operating bit SNR to achieve the desired probability of error. Let's also define $\mathbf{SNRb}_{\rm rec}(N_u) > \mathbf{SNRb}_{\rm spec}$ to be the required value of $\mathbf{SNRb}_{\rm out}(1)$ in (15) that makes $\mathbf{SNRb}_{\rm out}(N_u) = \mathbf{SNRb}_{\rm spec}$, so user one can still meet the specified value of bit error probability even when other N_u-1 users are active. Using the definitions above in (15) we get

$$\mathbf{SNRb}_{\rm spec} = \frac{\mathbf{SNRb}_{\rm rec}(N_u)}{1+\mathbf{SNRb}_{\rm rec}(N_u)\left[\frac{G}{\sum_{\nu=2}^{N_u}\left(\frac{A^{(\nu)}}{A^{(1)}}\right)^2}\right]^{-1}} \quad (17)$$

and from (17) we get

$$\mathbf{SNRb}_{\rm rec}(N_u) = \frac{\mathbf{SNRb}_{\rm spec}}{1-\mathbf{SNRb}_{\rm spec}\left[\frac{G}{\sum_{\nu=2}^{N_u}\left(\frac{A^{(\nu)}}{A^{(1)}}\right)^2}\right]^{-1}}.$$

The ratio

$$\mathrm{DF}(N_u) \triangleq \frac{\mathbf{SNRb}_{\rm rec}(N_u)}{\mathbf{SNRb}_{\rm spec}} \quad (18)$$

is a degradation factor that measures the additional amount of SNR required by user one to overcome the negative effect of the multiple-access interference caused by the other N_u-1 users.

It can be observed that, as N_u increases, $\mathrm{DF}(N_u)$ also increases, meaning that $\mathbf{SNRb}_{\rm rec}(N_u)$ must be increased in order to keep constant the right hand side of (17). Ultimately, however, no amount of increase in $\mathbf{SNRb}_{\rm rec}(N_u)$ can offset the increase in the other term. As a result, the number of users can be increased to a maximum number in which DF in (18) becomes infinity. On the other hand, note that $\mathbf{SNRb}_{\rm rec}(N_u) \to \mathbf{SNRb}_{\rm spec}$ as $N_u \to 1$, as would be expected with only one user active.

Under ideal power control conditions (i.e., when $A^{(\nu)} = A^{(1)}$ for $\nu = 2, 3, \ldots, N_u$), the $\mathrm{DF}(N_u)$ in (18) can be written

$$\mathrm{DF}(N_u) = \frac{1}{1-\mathbf{SNRb}_{\rm spec}\left[\frac{G}{(N_u-1)}\right]^{-1}}. \quad (19)$$

The expression in (19) gives DF as a function of N_u, and it can be used to find N_u as a function of DF as follows[4]

$$N_u(\mathrm{DF}) = \frac{1}{\mathbf{SNRb}_{\rm spec}} G\left(1-\frac{1}{\mathrm{DF}}\right)+1. \quad (20)$$

[4]Since N_u is an integer, $N_u(\mathrm{DF})$ in (20) is assigned the truncated value of the right hand side.

Type of signal	multiple-access bit SNR
OR	$\mathbf{SNRb}_{\rm OR}(N_u) = \frac{(A^{(1)})^2 E_b}{N_o + \sum_{\nu=2}^{N_u} N_{\rm OR}^{(\nu)}}$ $N_{\rm OR}^{(\nu)} = \frac{(A^{(\nu)})^2 E_b}{(\mu_{\rm OR}/T_f)/R_b}$ $\mu_{\rm OR} = \frac{m_w^2(0,0,T_{\rm OR})}{\sigma_w^2(0,T_{\rm OR})}$
EC	$\mathbf{SNRb}_{\rm EC}(N_u) = \frac{(A^{(1)})^2 E_b(1-\lambda)}{N_o + \sum_{\nu=2}^{N_u} N_{\rm EC}^{(\nu)}}$ $N_{\rm EC}^{(\nu)} = \frac{(A^{(\nu)})^2 E_b[1-\lambda]}{(\mu_{\rm EC}/T_f)/R_b}$ $\mu_{\rm EC} = \frac{m_w^2(0,0,\tau_2)}{2\sigma_w^2(0,\tau_2)}$
NO1	$\mathbf{SNRb}_{\rm NO1}(N_u) = \begin{cases} \mathbf{SNRb}_{\rm OR}(N_u), & \text{for } \lfloor \frac{j-1}{2} \rfloor \neq \lfloor \frac{i-1}{2} \rfloor \\ \mathbf{SNRb}_{\rm TSK}(N_u), & \text{for } \lfloor \frac{j-1}{2} \rfloor = \lfloor \frac{i-1}{2} \rfloor \end{cases}$ $\mathbf{SNRb}_{\rm TSK}(N_u) = \frac{(A^{(1)})^2 E_b(1-\gamma_w(\tau_2))}{N_o + \sum_{\nu=2}^{N_u} N_{\rm TSK}^{(\nu)}}$ $N_{\rm TSK}^{(\nu)} = \frac{(A^{(\nu)})^2 E_b[1-\gamma_w(\tau_2)]}{(\mu_{\rm TSK}/T_f)/R_b}$ $\mu_{\rm TSK} = \frac{m_w^2(0,0,\tau_2)}{\sigma_w^2(0,\tau_2)}$
NO2	$\mathbf{SNRb}_{\rm NO2}(N_u) = \begin{cases} \mathbf{SNRb}_{\rm OR}(N_u), & \text{for } \lfloor \frac{j-1}{2} \rfloor \neq \lfloor \frac{i-1}{2} \rfloor \\ \mathbf{SNRb}_{\rm EC}(N_u), & \text{for } \lfloor \frac{j-1}{2} \rfloor = \lfloor \frac{i-1}{2} \rfloor \end{cases}$

TABLE IV

MULTIPLE-ACCESS BIT SNR FOR THE FOUR DIFFERENT SIGNAL DESIGNS UNDER STUDY.

From (20) the maximum number of users is

$$N_{\max} \triangleq \lim_{\rm DF \to \infty} N_u({\rm DF}) = \frac{1}{\mathbf{SNRb}_{\rm spec}} G + 1. \quad (21)$$

The value $N_{\max}$ is the largest value that N_u can attain when the performance is determined by the amount of multiple-access interference produced by the other $N_u - 1$ active users.

The $N_{\max}$ can be used to define

$$C_{\max} \triangleq N_{\max} R_b \simeq \frac{(\mu/T_f)}{\mathbf{SNRb}_{\rm spec}}, \text{ (for } N_{\max} >> 1). \quad (22)$$

The $C_{\max}$ is the largest value that the total combined bit transmission rate $N_u R_b$ can attain, i.e., plays the role of *total multiple-access transmission capacity.*

The expression (21) clearly indicate that $N_{\max}$ can be increased by decreasing $\mathbf{SNRb}_{\rm spec}$. The limit on how small $\mathbf{SNRb}_{\rm spec}$ can be for a given number of users N_u is investigated in section IV-C.

C. The $N_{\rm sup}$ and $C_{\rm sup}$

In this section we study both $N_{\rm sup}$, the upper bound on the number of users N_u, and $C_{\rm sup}$, the upper bound on the total combined bit transmission rate $N_u R_b$, under ideal power control.

The expression for $C_{\rm sup}$ can be derived using Shannon's formula for channel capacity [18]

$$C(W) = W \log_2(1 + \frac{1}{W} {\rm PNR}), \quad (23)$$

where W is the 3 dB bandwidth occupied by the PPM signals (i.e. the 3 dB bandwidth of the pulse $w(t)$), and

Type of signal	multiple-access BER
OR	$\mathrm{UBP}_{\mathrm{b}}^{(\mathrm{OR})} = \frac{M}{2} Q\left(\sqrt{\log_2(M)\mathbf{SNRb}_{\mathrm{OR}}(N_u)}\right)$
EC	$\mathrm{UBP}_{\mathrm{b}}^{(\mathrm{EC})} = \frac{M}{2} Q\left(\sqrt{\log_2(M)\mathbf{SNRb}_{\mathrm{EC}}(N_u)}\right)$
NO1	$\mathrm{UBP}_{\mathrm{b}}^{(\mathrm{NO1})} = Q\left(\sqrt{\log_2(M)\mathbf{SNRb}_{\mathrm{TSK}}(N_u)}\right) + \frac{M-2}{2} Q\left(\sqrt{\log_2(M)\mathbf{SNRb}_{\mathrm{OR}}(N_u)}\right)$
NO2	$\mathrm{UBP}_{\mathrm{b}}^{(\mathrm{NO2})} = Q\left(\sqrt{\log_2(M)\mathbf{SNRb}_{\mathrm{EC}}(N_u)}\right) + \frac{M-2}{2} Q\left(\sqrt{\log_2(M)\mathbf{SNRb}_{\mathrm{OR}}(N_u)}\right)$

TABLE V

MULTIPLE-ACCESS BER $\mathrm{UBP}_{\mathrm{b}}$ FOR THE FOUR DIFFERENT SIGNAL DESIGNS UNDER STUDY.

$\mathrm{PNR} \triangleq R_b\, \mathbf{SNRb}_{\mathrm{spec}}$ is the *bit-power to noise-power density* ratio. The maximum value of PNR can be obtained using the maximum value of $\mathbf{SNRb}_{\mathrm{spec}}$. The later can be found if we let $\mathbf{SNRb}_{\mathrm{rec}}(N_u)$ take on large values in (17) to get

$$\begin{aligned} \mathbf{SNRb}_{\max}(N_u) &\triangleq \lim_{\mathbf{SNRb}_{\mathrm{rec}}(N_u)\to\infty} \mathbf{SNRb}_{\mathrm{spec}} \\ &= \frac{(\mu/T_f)/R_b}{(N_u-1)}. \end{aligned}$$

Hence

$$\begin{aligned} \mathrm{PNR}_{\max}(N_u) &\triangleq R_b \mathbf{SNRb}_{\max}(N_u) \\ &= \frac{(\mu/T_f)}{(N_u-1)}. \end{aligned} \tag{24}$$

Substituting (24) into (23), and expanding in power series, the maximum value of $C(W)$ for a given W can be written

$$C(W) = \frac{W}{\log_e(2)} \sum_{k=1}^{\infty} \frac{(-1)^{k+1}}{k} \left(\frac{1}{W}\frac{(\mu/T_f)}{N_u-1}\right)^k.$$

By letting $W \to \infty$ (i.e., by letting the width of the pulse $w(t)$ approach zero[5]) we have that

$$\lim_{W\to\infty} C(W) \simeq \frac{1}{\log_e(2)} \frac{(\mu/T_f)}{N_u-1} \triangleq R_{\mathrm{sup}}.$$

The R_{sup} is an upper bound on R_b, hence

$$C_{\max} < C_{\mathrm{sup}} \triangleq N_u R_{\mathrm{sup}} \simeq \frac{(\mu/T_f)}{\log_e(2)}, (N_u >> 1). \tag{25}$$

[5]Recall that C and $N_{\max}$ were derived for equally correlated signals. These signals are known to be optimal in the sense that they can achieve channel capacity (i.e, error free transmission under bit transmission constraints) as the number of the signals M approaches infinity [19]. As M approaches infinity the signal set requires unbounded time and bandwidth resources.

The C_{sup} in (25) gives an upper bound on the total combined bit transmission rate $N_u R_b$ that can can be attained when the performance is determined by the amount of multiple-access interference with N_u users active, each one transmitting at bit rate R_b.[6]

Using C_{sup} in(25) we can define

$$N_{\max} < N_{\mathrm{sup}} \triangleq \frac{C_{\mathrm{sup}}}{R_b} \simeq \frac{G}{\log_e(2)}, (N_u >> 1). \tag{26}$$

The N_{sup} in (26) is an upper bound on the number of active users N_u that the system can support for a given G. The N_{sup} agrees with the 'cocktail party effect', in which the number of users (or 'party guests talking simultaneously') is maximized when each user 'talks' as softly as possible, constrained to use $\mathbf{SNRb}_{\mathrm{spec}} > \log_e(2)$.

D. Discussion

The MA BER analysis in section IV-A compare BER for different values of M for a particular signal design. This analysis is meaningful when the comparison for different M is done keeping constant the values E_b and R_b, as well as the total bandwidth of the M-ary signals. Similarly, the number of users calculated in section IV-B for different values of M for EC PPM signals is meaningful when the comparison for different M is done keeping constant the values E_b and R_b, as well as the BER and the total bandwidth of the M-ary signals.

To have all M-ary systems operate at the same bit transmission rate R_b for different values of M, it is necessary to increase T_s as M increases. That is, a particular M-ary

[6]The fact that the upper bound in (25) depends on the signal design through μ/T_f is a consequence that the MA interference, assumed to be Gaussian in this analysis, also depends on the signal design.

system should use a block time T_s, given by

$$T_s \triangleq \frac{\log_2(M)}{R_b}, \tag{27}$$

However, this also mean that for a given M we have that

$$E_s = \log_2(M) E_b, \tag{28}$$

i.e., the M-ary symbol energy is $\log_2(M)$ times the bit energy E_b.

In our M-ary TH PPM system, the $\log_2(M)$ scaling in (27) and (28) can be obtained by defining the number of pulses N_s used in M-ary communications $N_s \triangleq \log_2(M) N_s^{(2)}$, where $N_s^{(2)}$ is the number of pulses used in binary communications. In this way $T_s = N_s T_f = \log_2(M) N_s^{(2)} T_f \triangleq \log_2(M)/R_b$, and $E_s = N_s E_w = \log_2(M) N_s^{(2)} E_w \triangleq \log_2(M) E_b$. Notice that this scaling does not a affect the total bandwidth of the M-ary signals, which is a function of the total bandwidth W of $w(t)$.

V. Numerical examples

A. Example 1: MA BER

In this section we illustrate the theoretical MA performance of this system for a specific $w(t)$ under perfect power control (i.e. $A^{(\nu)} = A^{(1)}$ for $\nu = 2, 3, \ldots, N_u$). The $w(t)$ considered here is the second derivative of a Gaussian function[7]

$$w(t) = \left[1 - 4\pi \left[\tfrac{t}{t_n}\right]^2\right] \exp\left(-2\pi \left[\tfrac{t}{t_n}\right]^2\right), \tag{29}$$

where the value t_n is used to fit the model $w(t)$ to a measured waveform from a particular experimental radio link. The normalized signal correlation function corresponding to $w(t)$ in (29) is

$$\gamma_w(\tau) = \left[1 - 4\pi \left[\tfrac{\tau}{t_n}\right]^2 + \tfrac{4\pi^2}{3}\left[\tfrac{\tau}{t_n}\right]^4\right] \exp\left(-\pi \left[\tfrac{\tau}{t_n}\right]^2\right).$$

In this case T_w and $\tau_{\min}$ depends on t_n, and $\gamma_{\min} = -0.6183$ for any t_n. Using $t_n = 0.4472$ ns we get $T_w \simeq 1.2$ ns and $\tau_{\min} \simeq 0.2419$ ns. Fig. 2 depicts $w(t - T_w/2)$, $\gamma_w(\tau)$ and the spectrum of $w(t)$. The 3 dB bandwidth of $w(t)$ is in excess of one GHz.

Given $w(t)$, the signal design is complete when we specify N_s, T_f and $\{\delta_j^k\}$ in table I. For OR signals $T_{\rm OR} = 2T_w$, for EC signals $\tau_1 = 0$ and $\tau_2 = \tau_{\min}$, for NO1 signals $\tau_1 = 0$, $\tau_2 = \tau_{\min}$ and $T_{\rm NO1} = \tau_{\min} + 2T_w$, and for NO2 signals $\tau_1 = 0$, $\tau_2 = \tau_{\min}$ and $T_{\rm NO2} = \tau_{\min} + 2T_w$.

To chose a value for T_f, notice that condition (f) in section II-E requires $0 < N_h T_c < (T_f/2) - 2(T_w + \tau_\eta)$. Also notice that $\tau_\eta = 16 T_{\rm OR}$ for $M = 16$ (the maximum value of M in this example). By choosing $T_f = 100$ ns we have that $0 < N_h T_c < 16$ ns.

To choose a value for N_s, notice that the M-ary PPM signal designs considered in [10] require that $N_s = 1/(R_s T_f) = \log_2(M)/(R_b T_f) = \log_2(M) N_s^{(2)}$. Hence, for a fixed T_f, the value of N_s is determined by R_b. However, in particular the EC PPM signal design additionally requires $N_s \geq M$. Combining this two requirements on N_s we have that in the EC PPM case both R_b and N_s satisfy the relation $(\log_2(N_s)/N_s) \geq R_b T_f$. In this example we use $R_b = 100$ kilobits per second, $N_s^{(2)} = 100$, $2 \leq M \leq 16$ and $N_s = \log_2(M)100$, hence $(\log_2(N_s)/N_s) \geq R_b T_f$ holds, and both relations $N_s \geq M$ and $N_s = \log_2(M)/(R_b T_f)$ are satisfied.

Once the signal design is completed, we can evaluate $\mathbf{SNRb}_{\rm OR}$, $\mathbf{SNRb}_{\rm EC}$, $\mathbf{SNRb}_{\rm NO1}$ and $\mathbf{SNRb}_{\rm NO2}$ in table IV. Fig. 3 depicts the MA performance curves for $\mathrm{UBP}_{\rm b}^{(\rm OR)}(N_u)$, $\mathrm{UBP}_{\rm b}^{(\rm EC)}(N_u)$, $\mathrm{UBP}_{\rm b}^{(\rm NO1)}(N_u)$ and $\mathrm{UBP}_{\rm b}^{(\rm NO2)}(N_u)$ in table V, respectively. In all cases we used an single-link communications output bit $E_b/N_o = 14.30$ dB, hence $\mathbf{SNRb}_{\rm OR}(1) = 14.30$ dB, $\mathbf{SNRb}_{\rm EC}(1) = 13.39$ dB and $\mathbf{SNRb}_{\rm TSK}(1) = 16.40$ dB.

B. Example 2: N_u

In this example we evaluate $N_u(\mathrm{DF})$ in (20) using the same EC PPM signal design used in Example 1, i.e, we use the pulse $w(t)$ in (29), $t_n = 0.4472$ ns, $T_w = 1.2$ ns, $\tau_{\min} = 0.2419$ ns, $\tau_1 = 0$, $\tau_2 = \tau_{\min}$, and $T_f = 100$ ns. Fig. 4 shows $N_u(\mathrm{DF})$ for different values of DF using $R_b = 100$ kilobits per second, $N_s^{(2)} = 100$, $2 \leq M \leq 256$ and $N_s = \log_2(M)100$. Notice that $(\log_2(N_s)/N_s) \geq R_b T_f$ still holds for $M = 256$.

From $N_u(\mathrm{DF})$ in (20) we can also find $R_b(\mathrm{DF})$ for a particular value of N_u. Fig. 5 shows $R_b(\mathrm{DF})$ for different values of DF using $N_u = 1000$ active users.

C. Example 3: $N_{\rm sup}$, $C_{\rm sup}$ and G

In this example we evaluate $N_{\rm sup}$ in (26), $C_{\rm sup}$ in (25) and G in (16). This requires the evaluation of $\mu = \mu_{\rm EC}^{(2)}$. For this purpose we define a *binary* signal design using the same EC PPM signal design used in Examples 1 and 2, i.e, we use the pulse $w(t)$ in (29), $t_n^{(2)} = 0.4472$ ns, $T_w^{(2)} = 1.2$ ns, $\tau_{\min}^{(2)} = 0.2419$ ns, $\tau_1^{(2)} = 0$, $\tau_2^{(2)} = \tau_{\min}^{(2)}$, and $T_f^{(2)} = 100$ ns. The value of $\mu = \mu_{\rm EC}^{(2)}$ can then be calculated from table IV and (10) and (9).

The value of μ was calculated for three different pulse width parameters $t_n^{(I)}$, $t_n^{(II)}$ and $t_n^{(III)}$. These values are shown in table VI, together with the respective values of $C_{\rm sup}$. Also included are the values of G and $N_{\rm sup}$ calculated using $R_b = 100$ Kilo bits per second (Kbps). The superscript (i), $i = I, II, III$ denotes a quantity calculated using set i of parameters.

From $C_{\rm sup}$ in (25) we can also find $R_{\rm sup}$ as a function of N_u. Fig. 6 shows $R_{\rm sup}(N_u)$ calculated using the parameters in table VI.

VI. Conclusion

From Fig. 3 the benefits of using block waveform modulation are evident. By using higher values of M other than 2, it is possible either to improve the probability of detection for a fixed number of users N_u, or to increase the

[7] The $w(t)$ in (29) is one possible model for the ultra-wideband impulse $w(t)$ used in impulse radio modulation [2].

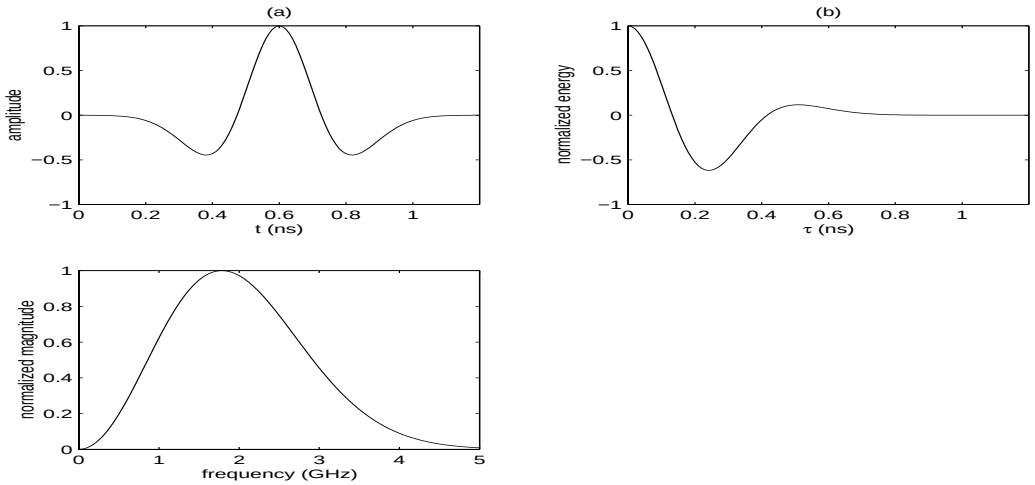

Fig. 2. (a) The pulse $w(t - T_w/2)$ as a function of time t. (b) The signal autocorrelation function $\gamma_w(\tau)$ as a function of time shift τ. (c) The magnitude of the spectrum of the pulse $w(t)$.

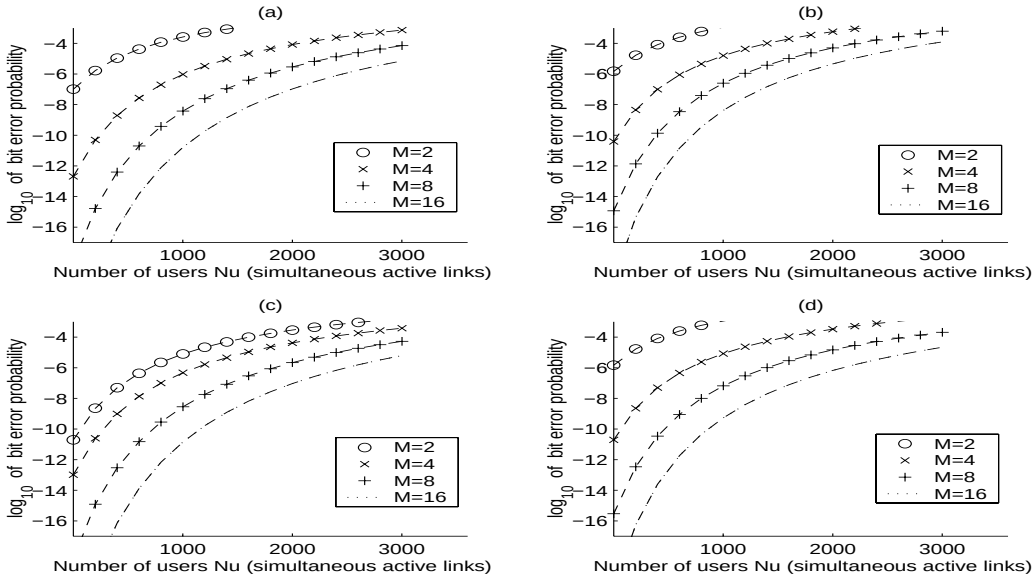

Fig. 3. The base 10 logarithm of the probability of bit error as a function of N_u for different values of M, using $R_b = 100$ Kbps. (a) OR PPM signals, $\mathbf{SNRb}_{\mathrm{OR}}(1) = 14.30$ dB. (b) EC PPM signals, $\mathbf{SNRb}_{\mathrm{EC}}(1) = 13.39$ dB. (c) NO PPM signals, design 1, $\mathbf{SNRb}_{\mathrm{OR}}(1) = 14.30$ dB and $\mathbf{SNRb}_{\mathrm{TSK}}(1) = 16.40$ dB. (d) NO PPM signals, design 2, $\mathbf{SNRb}_{\mathrm{OR}}(1) = 14.30$ dB and $\mathbf{SNRb}_{\mathrm{EC}}(1) = 13.39$ dB.

number of users for a fixed probability of error, without increasing each user's signal power. It can be verified that the benefit in going from one value of M to the next value actually decreases as M increases. The observer reader can verify that that for the particular signal designs in the example $\mathrm{UBP}_{\mathrm{b}}^{(\mathrm{NO1})} < \mathrm{UBP}_{\mathrm{b}}^{(\mathrm{OR})} < \mathrm{UBP}_{\mathrm{b}}^{(\mathrm{NO2})} < \mathrm{UBP}_{\mathrm{b}}^{(\mathrm{EC})}$, i.e., NO signals, design 1, rank first, OR signals rank second, NO signals, design 2, rank third and EC signals, rank fourth in terms of multiple-access performance. This is expected, since the signal sets can be ranked, in that order, in terms of favorable correlation properties.

Fig. 4 illustrates how by using higher values of M with fixed values for both the bit transmission rate and the probability of bit error, it is possible to increase the maximum number of users $N_{\max} = 739$ using $M = 2$ to $N_{\max} = 4141$ using $M = 256$. These values corresponds to $C_{\max} = 73.9$ Mega bps (Mbps) and $C_{\max} = 414.1$ Mbps, respectively. Similarly, Fig. 4 illustrates how for a fixed number of active users $N_u = 1000$ it is possible to increase the maximum transmission rate per user $R_{\max} = 73.9$ Kbps using $M = 2$ to $R_{\max} = 414.4$ Kbps using $M = 256$. Both Figs. 4 and 5 show that increasing DF beyond 10 dB provides a diminishing return, therefore a good system should be designed to work with DF ≤ 10 dB.

Table VI clearly indicates that for the upper bound on the total combined bit transmission rate we have that $C_{\mathrm{sup}}^{(I)}(N_u) > C_{\mathrm{sup}}^{(II)}(N_u) > C_{\mathrm{sup}}^{(III)}(N_u)$. Similarly, for the spreading gain factor we have that $G^{(I)} > G^{(II)} > G^{(III)}$.

set I of parameters	set II of parameters	set III of parameters
$t_n = 0.2877$ ns $T_w = 0.75$ ns $\tau_{\min} = 0.1556$ ns	$t_n = 0.4472$ ns $T_w = 1.2$ ns $\tau_{\min} = 0.2419$ ns	$t_n = 0.7531$ ns $T_w = 2.0$ ns $\tau_{\min} = 0.4073$ ns
$\mu^{(I)} = 252.27$ $C_{\text{sup}}^{(I)} = 3.6394$ (Gbps)	$\mu^{(II)} = 162.28$ $C_{\text{sup}}^{(II)} = 2.3412$ (Gbps)	$\mu^{(III)} = 96.37$ $C_{\text{sup}}^{(III)} = 1.3903$ (Gbps)
$G^{(I)} = 25227$ $N_{\text{sup}}^{(I)} = 36394$ (users)	$G^{(II)} = 16228$ $N_{\text{sup}}^{(II)} = 23412$ (users)	$G^{(III)} = 9637$ $N_{\text{sup}}^{(III)} = 13903$ (users)

TABLE VI

VALUES OF μ AND C_{sup} IN GIGA BPS (GBPS) CALCULATED USING THREE DIFFERENT PULSE WIDTHS. ALSO INCLUDED ARE THE VALUE OF G AND N_{sup} FOR $R_b = 100$ KBPS.

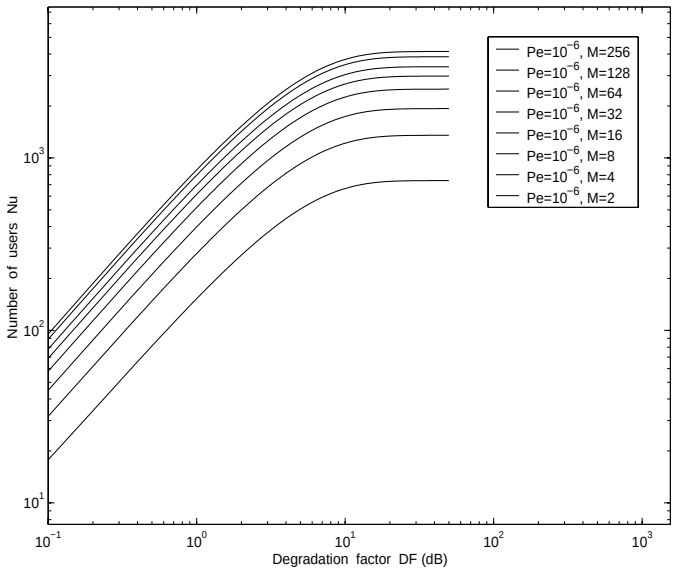

Fig. 4. The number of simultaneous active links (users) $N_u(\text{DF})$ for EC PPM signals for $2 \leq M \leq 256$ with $P_e(1) = \text{UBP}_{\text{b}}^{(\text{EC})}(1) \simeq 10^{-6}$ and $Rb = 100$ Kbps.

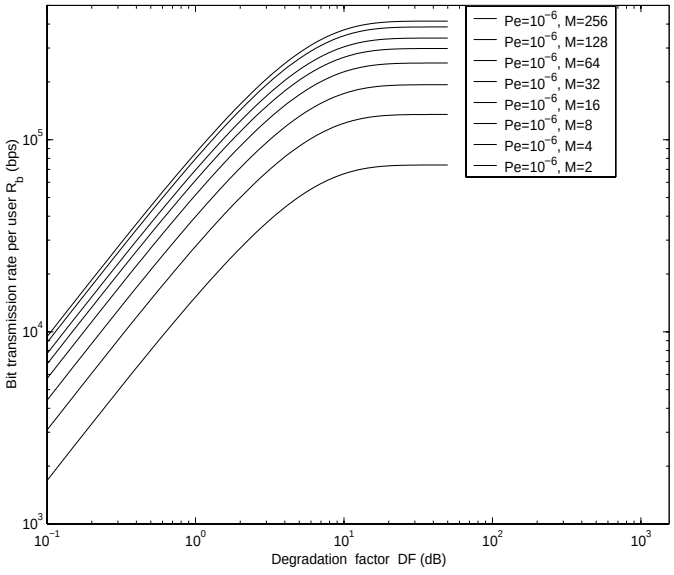

Fig. 5. The data transmission rate per user $R_b(\text{DF})$ for EC PPM signals for $2 \leq M \leq 256$ with $P_e(1) = \text{UBP}_{\text{b}}^{(\text{EC})}(1) \simeq 10^{-6}$ and $N_u = 1000$ active users.

This is to be expected since the "more impulsive" the signals are, the less likely collisions among TH-PPM signals corresponding to different users are. In fact, the expression for the processing gain G can be manipulated to make it explicitly dependent on the ratio (T_f/T_w).

This analysis shows that impulse radio modulation is theoretically able to provide multiple-access communications in a Gaussian Channel with a combined transmission capacity of hundreds of Megabits per second at bit error rates in the range 10^{-4} to 10^{-7} using receivers of moderate complexity. The validity of the analysis is ensured as long as the conditions stated in section II-E are satisfied. The use of the union bound in this theoretical analysis is justified for the values of signal to noise ratio used in the examples. This analysis, combined with simulations using non-random time hopping patterns, should give calculations that reflect the performance attainable in practical systems under similar conditions.

For communications in the presence of multipath, the greatest potential for impulse radio modulation comes from the fine time resolution produced by the subnanosecond

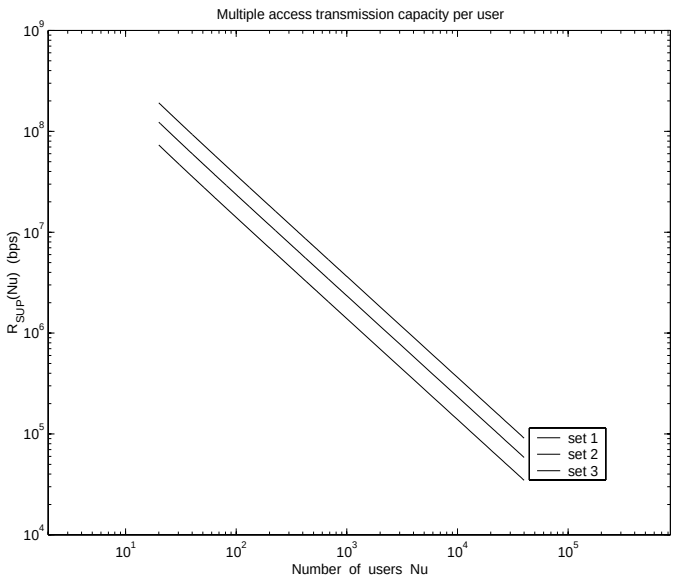

Fig. 6. Upper bound on the bit transmission rate per user $R_{\sup}(N_u)$ in bps, calculated using the sets I, II, III of parameters in table VI.

pulses. Propagation paths with differential delays in the order of this pulse width or more can be resolved and coherently combined using a Rake receiver, hence combating the normally degrading effects of multipath. For a single user using impulse radio modulation, one study [20] has shown that the fading margin can be as low as 1.5 dB. Further studies are needed to asses the multiple-access performance of impulse radio modulation in the presence of multipath.

VII. Acknowledgments

The author is very grateful to Dr. Robert A. Scholtz for his advice during this research endeavor. He also wants to give special thanks to the anonymous reviewers whose comments helped to improve the quality of this paper.

References

[1] P. Withington II and L. W. Fullerton, "An impulse radio communications system," in *Ultra-Wideband, Short-Pulse Electromagnetics,* H. L. Bertoni, L. Carin and L. B. Felson, Ed. New York: Plenum Press, 1993, pp. 113-120.

[2] R. A. Scholtz, "Multiple access with time hopping impulse modulation," invited paper, in *Proc. IEEE MILCOM Conf.*, pp. 447-450, December 1993.

[3] J. Lindner, "The performance of code division multiplexing with pulse position modulation," in *Proc. NATO AGARD Conf.* , no. 239, pp. 35-1 trough 35-11, 1979.

[4] I. Okazaki and T. Hasegawa, "Spread spectrum pulse position modulation - A simple approach for Shannon's limit," *IEICE Trans. Commun.*, vol. E76-B, no. 8, pp. 929-940, August 1993.

[5] U.S. patent 5812081: *Time domain radio transmission system.*

[6] M. Z. Win and R. A. Scholtz, "Impulse radio: How it works?," *IEEE Commun. Letters,* vol. 2, no. 2, pp. 36-38, February 1998.

[7] F. Ramírez-Mireles and R. A. Scholtz, "System performance of impulse radio modulation," in *Proc. IEEE RAWCON Conf.*, pp. 67-70, August 1998.

[8] C. L. Weber, G. K. Huth and B. H. Batson, "Performance considerations of code division multiple-access systems," *IEEE Trans. on Veh. Technol.*, vol. VT-30, No. 1, pp 3-9, February 1981.

[9] F. Ramírez-Mireles and R. A. Scholtz, "Multiple access with time hopping and block waveform PPM modulation," in *Proc. IEEE ICC Conf.*, pp. 775-779, June 1998.

[10] F. Ramírez-Mireles, *Multiple-Access with Ultra-Wideband Impulse Radio Modulation Using Spread Spectrum Time-Hopping and Block Waveform Pulse-Position-Modulated Signals,* Ph.D. dissertation, Communication Sciences Institute, Electrical Engineering Department, University of Southern California, 1998.

[11] C. N. Georghiades, "On PPM sequences with good autocorrelation properties," *IEEE Trans. Inform. Theory*, vol. 34, no. 3, pp. 571-576, May 1988.

[12] R. Gagliardi, J. Robbins and H. Taylor, "Acquisition sequences in PPM communications," *IEEE Trans. Inform. Theory*, vol. 33, no. 5, pp. 738-744, September 1987.

[13] S. W. Golomb, "Construction of signals with favorable correlation properties," in *Surveys in Combinatorics,* London Mathematical Society Lecture Notes Series 166, Cambridge University Press, 1991.

[14] H. V. Poor, "Signal processing for wideband communications," *IEEE Information Society Newsletter*, June 1992.

[15] S. Verdu, "Recent progress in multiuser detection", in *Multiple Access Communications: Foundations for Emerging Technologies,"* IEEE Press, 1993, pp. 164-175.

[16] R. M. Gagliardi, *Introduction to Telecommunications Engineering,* John Wiley and Sons, 1988, pp. 357-437.

[17] H. Stark and J. W. Woods, *Probability, Random Processes, and Estimation Theory for Engineers,* Prentice Hall, 1986, pp. 143-146.

[18] C. E. Shannon, "A Mathematical theory of communication," *Bell Syst. Tech. J.*, vol. 27, July and October, 1948.

[19] M. K. Simon, S. H. Hinedi and W. C. Lindsey, *Digital Communication Techniques,* Prentice Hall, 1996, pp. 752-825.

[20] F. Ramírez-Mireles, "On performance of ultra wideband signals in Gaussian noise and dense multipath," accepted for publication in *IEEE Trans. on Veh. Technol.*

Fernando Ramírez-Mireles (M'88) received the B.S.E.E. from the Metropolitan Autonomous University (UAM), México, the M.S.E.E. from the Center for Advanced Studies of IPN (CINVESTAV), México, and the Ph.D.E.E. from the University of Southern California (USC), Los Angeles, CA.

He has worked for the Mexican Telephone Company and CINVESTAV, and also consulted for the National Bank of México. He was a Research Assistant at USC's Communication Sciences Institute, where he worked on ultra wideband (UWB) communications. In the summer of 1997 he was a MTS at Torrey Science Corp., San Diego, CA, where he worked on spread spectrum LEO satellite Communications. From 1998 to 1999 he was a MTS at Glenayre Technologies, Santa Clara, CA, where he worked on definition of demodulation architectures for NPCS mobile terminal. Presently, he is a MTS at Aware, Inc., Lafayette, CA, working on technology development for current and future standards of DSL.

He has published 16 technical articles in areas including modulation and signal design for UWB communications, spread spectrum multiple access performance, performance in multipath channels and speech recognition. He has one U.S. patent pending on DSL.

Dr. Ramírez-Mireles was a Fulbright Scholar while studying his Ph.D. program at USC. In México, he won an honorific Mention in the IV Ericsson's National Prize of Science and Technology, and received the Medal to the Universitarian Merit. He is a member of Tau Beta Pi.